














Mixotrophic growth of the extremophile *Galdieria sulphuraria* reveals the flexibility of its carbon assimilation metabolism

Gilles Curien¹ , Dagmar Lyska² , Erika Guglielmino¹, Phillip Westhoff², Janina Janetzko², Marianne Tardif³ , Clément Hallopeau¹ , Sabine Brugière³ , Davide Dal Bo¹, Johan Decelle¹ , Benoit Gallet⁴ , Denis Falconet¹ , Michele Carone⁵ , Claire Remacle⁵ , Myriam Ferro³ , Andreas P.M. Weber²  and Giovanni Finazzi¹ 

¹Laboratoire de Physiologie Cellulaire et Végétale, Université Grenoble Alpes, CNRS, CEA, INRAe, Grenoble Cedex 9 38054, France; ²Institute of Plant Biochemistry, Cluster of Excellence on Plant Sciences (CEPLAS), Heinrich Heine University, Düsseldorf 40225, Germany; ³EduP Laboratoire Biologie à Grande Echelle, Université Grenoble Alpes, CEA, Inserm, BGE U1038 Grenoble Cedex 9 38054, France; ⁴Institut de Biologie Structurale, Université Grenoble Alpes, CNRS, CEA, 71 Avenue des Martyrs Grenoble 38044, France; ⁵Genetics and Physiology of Microalgae, InBios/Phytosystems Research Unit, University of Liege, Liège 4000, Belgium

Summary

Author for correspondence:

Gilles Curien

Email: gilles.curien@cea.fr

Received: 13 November 2020

Accepted: 18 March 2021

New Phytologist (2021) 231: 326–338

doi: 10.1111/nph.17359

Key words: *Galdieria sulphuraria*, mixotrophy, photorespiration, photosynthesis, red algae.

- *Galdieria sulphuraria* is a cosmopolitan microalga found in volcanic hot springs and calderas. It grows at low pH in photoautotrophic (use of light as a source of energy) or heterotrophic (respiration as a source of energy) conditions, using an unusually broad range of organic carbon sources. Previous data suggested that *G. sulphuraria* cannot grow mixotrophically (simultaneously exploiting light and organic carbon as energy sources), its photosynthetic machinery being repressed by organic carbon.
- Here, we show that *G. sulphuraria* SAG21.92 thrives in photoautotrophy, heterotrophy and mixotrophy. By comparing growth, biomass production, photosynthetic and respiratory performances in these three trophic modes, we show that addition of organic carbon to cultures (mixotrophy) relieves inorganic carbon limitation of photosynthesis thanks to increased CO₂ supply through respiration. This synergistic effect is lost when inorganic carbon limitation is artificially overcome by saturating photosynthesis with added external CO₂.
- Proteomic and metabolic profiling corroborates this conclusion suggesting that mixotrophy is an opportunistic mechanism to increase intracellular CO₂ concentration under physiological conditions, boosting photosynthesis by enhancing the carboxylation activity of Ribulose-1,5-bisphosphate carboxylase-oxygenase (Rubisco) and decreasing photorespiration.
- We discuss possible implications of these findings for the ecological success of *Galdieria* in extreme environments and for biotechnological applications.

Introduction

The unicellular red alga *Galdieria sulphuraria* belongs to the Cyanidiophyceae, a class that includes five species often flourishing in different extreme environments (Merola *et al.*, 1981; Gross *et al.*, 1998; Gross & Oesterhelt, 1999; Oesterhelt *et al.*, 2007). From a phylogenetic perspective, plastids of the red algae gave rise to the complex plastids of, e.g. diatoms via secondary endosymbiosis (Yoon *et al.*, 2002, 2004; Bhattacharya *et al.*, 2003). Like other members of this class (Doemel & Brock, 1971; Reeb & Bhattacharya, 2010) *G. sulphuraria* has an extremophile lifestyle, withstanding low pH (pH optimum at 2) and elevated temperatures (up to 56°C). It thrives in soils and forms biotopes on rocks surrounding hot springs, fumaroles, or acid mining sites and even on burning coal spoil heaps (Moreira *et al.*, 1994; Gross *et al.*, 1998; Castenholz & McDermott, 2010; Barcyté *et al.*, 2018). Some mesophilic

species have been isolated from environments with moderate temperatures and/or a neutral pH (Gross *et al.*, 2002; Yoon *et al.*, 2006; Azúa-Bustos *et al.*, 2009; Iovinella *et al.*, 2018). Genome analysis (Barbier *et al.*, 2005; Schonknecht *et al.*, 2013; Rossoni *et al.*, 2019a) has pinpointed a very high metabolic flexibility of this alga, which is confirmed by its ability to grow in photoautotrophy (exclusive use of light as an energy source) and heterotrophy (organic carbon respiration of more than 50 different substrates (Gross & Schnarrenberger, 1995)). This capacity, along with the peculiar pH optimum for growth, allow *G. sulphuraria* to be cultivated in open ponds containing organic matter, overcoming other microorganisms, considered as contaminants in this case. Given these advantages for large-scale cultivation, *G. sulphuraria* is considered an emerging system for biotechnology applications (Schmidt *et al.*, 2005; Henkanatte-Gedera *et al.*, 2017; Cizkova *et al.*, 2019).

The relationship between photosynthesis and glycolysis/respiration in higher plants and microalgae is complex (Avelange *et al.*, 1988; Kromer *et al.*, 1988; Gemel & Randall, 1992; Pärnik & Keerberg, 1995; Hoefnagel *et al.*, 1998; Tcherkez *et al.*, 2008). Photosynthesis/glycolysis/respiration interactions are prone to perturbation by mixotrophy, in which external organic carbon often interferes with carbon flow between chloroplasts, the cytosol and mitochondria. Several green microalgae are capable of mixotrophic growth (Combres *et al.*, 1994; Wan *et al.*, 2011; Johnson & Alric, 2012; Cecchin *et al.*, 2018). While mixotrophy has always beneficial consequences on respiration, its effects on photosynthesis differ depending on the microalga considered: enhancement of photosynthesis was reported in one case (*Ettlia oleoabundans* (Ferroni *et al.*, 2018)), while in other algae, including the diatoms *Phaeodactylum tricornutum* (Liu *et al.*, 2009; Villanova *et al.*, 2017) and *Nannochloropsis* (Fang *et al.*, 2004; Xu *et al.*, 2004) photosynthesis was unaffected. Decreased photosynthetic activity in mixotrophy has been reported in *Chlorella vulgaris* (Martinez & Orus, 1991; Cecchin *et al.*, 2018) and *Chlamydomonas reinhardtii* where the carbon concentrating mechanism (CCM (Bogaert *et al.*, 2019)) and the light harvesting capacity (Perrineau *et al.*, 2014) is decreased by acetate along with the enhancement of respiration. While it has been reported that *G. sulphuraria* 074G could grow in the simultaneous presence of light and a carbon source, heterotrophy seemed to prevail in these conditions, as no photosynthetic oxygen (O_2) production could be measured in the presence of glucose (Oesterheld *et al.*, 2007).

Here, we show instead that photosynthesis and carbon metabolism (glycolysis and respiration) operate simultaneously in *Galdieria sulphuraria* SAG21.92 (a close relative of the 074G strain) under mixotrophic conditions, provided that the temperature conditions are kept close to the ones experienced by this alga in its natural environment. We show that performances in mixotrophy, exemplified by photosynthetic activity and biomass production, actually exceed the sum of the heterotrophic and photoautotrophic yields under limiting inorganic carbon. This synergistic effect stems from a stimulation of photosynthesis by CO_2 of respiratory origin, which overcomes the limitation to the Calvin–Benson–Bassham cycle and suppresses photorespiration.

Limitation originates from the very low inorganic carbon concentration available in acidic conditions (pH 2) that constitute the alga's natural growth environment. Notably, under these conditions, inorganic carbon is almost exclusively available as dissolved CO_2 (around $10\ \mu M$) while soluble bicarbonate is virtually absent. Consistent with this hypothesis, the synergistic effect of 'light' and 'dark' energetic metabolisms is sensitive to respiration inhibitors and is lost upon addition of exogenous CO_2 , which outcompetes endogenous CO_2 of respiratory origin in relieving inorganic carbon limitation of the Calvin–Benson–Bassham cycle. We conclude that mixotrophy constitutes an efficient mechanism to increase intracellular CO_2 concentration under physiological conditions, allowing *G. sulphuraria* to successfully exploit all the energy resources available for growth in its rather challenging environment.

Materials and Methods

Strains, growth and media composition

Galdieria sulphuraria SAG21.92 and 074G were obtained from the Culture Collection of Algae at Göttingen University (SAG), Germany, and were grown in sterile $2 \times GS$ modified Allen medium, pH 2.0, containing 20 mM of sodium nitrate ($NaNO_3$), and 5 mM of inorganic phosphate (K_2HPO_4 and KH_2PO_4 in a 2 : 1 ratio (Allen, 1959)) at $42^\circ C$ without or with organic substrates as indicated in the text. The concentration of organic substrates was selected on the basis of data reported in the literature (Oesterheld *et al.*, 2007). More precisely, glucose was employed at the concentration of 25 mM, as in Oesterheld *et al.* (2007). The concentration of all the other organic compounds was adjusted to reach the same carbon atom concentration (150 mM). *Galdieria sulphuraria* was grown either in 250 ml flasks (50 ml culture volume), in an incubator (Infors, Bottmingen-Basel, Switzerland, continuous light, $30\ \mu mol\ photons\ m^{-2}\ s^{-1}$, $42^\circ C$, 100 rpm) or in a photobioreactor (Multicultivator; Photon System Instruments, Drásov, Czech Republic). Inside the multicultivator, cells were provided with air or CO_2 -enriched air by active bubbling (see Supporting Information Methods S1). Moreover, the incident light intensity was adjusted daily to maintain constant transmitted light through the culture (see Results section). This 'luminostat' regime ensures maximal absorption of light without allowing a dark zone to develop inside the photobioreactor (Cuaresma *et al.*, 2011). Growth was monitored daily by cell counting with a LUNA cell counter (Logos Biosystems Inc., Annandale, VA, USA). Sorbitol consumption was measured using the D-sorbitol/xylitol assay kit (Megazyme, Bray, Ireland).

Cell fresh weight and dry weight quantification

Cell pellet was resuspended in a small volume of water and centrifuged in pre-weighed Eppendorf tubes and the pellet was weighed. For dry weight determination fresh cell pellets were dried for three days at $60^\circ C$, weighed and expressed as $g\ l^{-1}$.

Clark electrode oxygen measurements

Oxygen exchanges in solution were measured with a Clark-type electrode (Hansatech Instruments, King's Lynn, UK) at $42^\circ C$. Respiration and gross photosynthesis were quantified by measuring the slope of O_2 changes in the dark and under light exposure, respectively. Net photosynthesis was calculated assuming O_2 consumption by the mitochondrion in the light is identical to that in the dark (Net photosynthesis = $\nu_{O2light} + |\nu_{O2dark}|$).

Photophysiology measurements

Photosynthetic parameters were derived from quantification of chlorophyll fluorescence emission by cultures within the multicultivator. To this aim, we employed a custom-made fluorescence imaging system based on a previously published setup (Johnson

et al., 2009) modified as described in Methods S1. The photosynthetic electron transfer rate (ETR) (a proxy of the carbon assimilation capacity (Maxwell & Johnson, 2000)) was calculated as $(F_m' - F_s)/F_m' \times \text{PFD}$, where F_m' and F_s are the fluorescence intensities measured after exposure to a saturating pulse and in steady state, respectively, in light-acclimated cells and PFD (photosynthetic flux density) is the incident light intensity, measured in $\mu\text{mol photons m}^{-2} \text{s}^{-1}$. The cells were allowed to reach steady-state fluorescence emissions at each intensity (5–10 min of light exposure depending on the intensity) before increasing the photon flux.

Biochemistry and proteomic analysis

Western blot analysis was performed on cells grown for 7 d in the indicated conditions. Cells (10^9 cells) were broken with a Precellys homogenizer (Bertin, Beaumont-Village, France), through three cycles of 30 s at 10 000 rpm separated by a 30-s interval. Total protein extracts were analyzed by immunoblotting with an anti-Ribulose-1,5-bisphosphate carboxylase-oxygenase (anti-Rubisco) antibody (Agrisera, Vännäs, Sweden). An antibody against the β subunit of the ATP synthase complex (Agrisera) was used as a loading control. 10 μg of protein was loaded per well.

For proteomic analysis, algae were cultivated under the three conditions photoautotrophy, mixotrophy and heterotrophy in parallel in the same cultivator. Three multicultivator experiments were carried out one week apart and constituted the three independent biological replicates. Cells were collected on day 7 (i.e. 4 d after addition of 25 mM D-sorbitol to mixotrophic and heterotrophic cultures). Proteins from whole cell extracts (40 μg each) were solubilized in Laemmli buffer before being stacked in the top of a 4–12% NuPAGE gel (Life Technologies, Waltham, MA, USA), stained with R-250 Coomassie blue (Bio-Rad, Hercules, CA, USA) and in-gel digested using modified trypsin (sequencing grade; Promega, Madison, WI, USA) as previously described (Bouchnak *et al.*, 2019). Resulting peptides were analyzed by online nanoLC-MS/MS (Ultimate 3000 RSLCnano coupled to Q-Exactive HF; ThermoFisher Scientific, Waltham, MA, USA) using a 200-min gradient. Peptides and proteins were identified using MASCOT (v.2.6.0, Matrix Science). Spectra were searched against Uniprot (*G. sulphuraria* taxonomy, July 2019 version, 7347 sequences) concomitantly with a home-made list of contaminants frequently observed in proteomics analyses (trypsin and keratins, 250 sequences).

The PROLINE software (Bouyssié *et al.*, 2020) was used to filter the results (conservation of rank 1 peptides, peptide identification false discovery rate (FDR) < 1% as calculated on peptide scores by employing the reverse database strategy, minimum peptide score of 25, and minimum of one specific peptide per identified protein group). Proline was then used to extract the MS1-based intensities values of protein groups from unique peptides. Proteins identified in the reverse and contaminant databases (i.e. trypsin or keratin), and proteins identified with only one peptide with a score < 40 were further discarded from the list. Proteins identified in only one or two conditions were kept for analysis without statistical treatment. Proteins identified in all three

conditions were submitted to statistical differential analysis using PROSTAR (Wieczorek *et al.*, 2017; Wieczorek *et al.*, 2019). Detailed procedures are described in Methods S1.

Metabolite extraction and analysis

Cells grown in a multicultivator were harvested at day 5 by centrifugation (4°C, 5 min and 3000 rcf), washed with ice-cold 0.9 % (w/v) sodium chloride (NaCl), snap frozen in liquid nitrogen, and lyophilized overnight. Cells (5×10^8) were disrupted in a Mixer Mill (MM 400; Retsch GmbH, Haan, Germany) for 60 s at 30 Hz using metal beads and 500 μl of ice-cold chloroform and methanol (1 : 2.3 ratio; containing 5 μM Ribitol and 2,4-dimethylphenylalanine (both from Sigma-Aldrich, Munich, Germany) as internal standards) with another round of shaking in the Mixer Mill. After a 2 h incubation at -20°C , 400 μl of ice-cold deionized water (Milli Q; Merck Chemicals GmbH, Darmstadt, Germany) were added to induce phase separation. The samples were vortexed and centrifuged for 5 min at 4°C and 16 000 rcf. The aqueous phase was transferred to a new reaction tube and the organic phase was re-extracted with 400 μl of ice-cold deionized water. Aqueous phases of each sample were combined and lyophilized overnight. After resuspension in 500 μl of 50% methanol 50 μl were dried in a glass inlet for analysis by gas chromatography-mass spectrometry (GC-MS) and ion chromatography-mass spectrometry (IC-MS).

For GC-MS analysis the samples were prepared and analyzed as described by Gu *et al.* (2012) and Shim *et al.* (2020). Identification of metabolites was performed with MASSHUNTER Qualitative (v.b08.00; Agilent Technologies, Santa Clara, CA, USA) by comparing spectra to the NIST14 Mass Spectral Library (<https://www.nist.gov/srd/nist-standard-reference-database-1a-v14>) and to a quality control sample containing all target compounds. Peaks were integrated using MASSHUNTER Quantitative (v.b08.00; Agilent Technologies). For relative quantification, all metabolite peak areas were normalized to the peak area of the internal standard ribitol.

For IC-MS a combination of a Dionex ICS-6000 HPIC and a high field Thermo Scientific Q Exactive Plus quadrupole-Orbitrap mass spectrometer following the method described in Schwaiger *et al.* (2017) and in Methods S1. Data analysis was conducted using COMPOUND DISCOVERER (v.3.1, ThermoFisher Scientific). Setting parameters for the untargeted metabolomics workflow and peak annotation criteria are described in Methods S1.

Labeling experiments with ^{13}C -glucose

Cells were cultivated in 250 ml Erlenmeyer flasks (50 ml culture volume) for 4 d under continuous light at $60 \mu\text{mol m}^{-2} \text{s}^{-1}$, 40°C and ambient air (0.04% CO_2). $\text{U-}^{13}\text{C}_6$ -glucose (Cambridge Isotope Laboratories Inc., Tewksbury, MA, USA) was added at day 4 in a final concentration of 25 mM and the irradiance was increased to $100 \mu\text{mol m}^{-2} \text{s}^{-1}$ either under ambient or elevated (2%) CO_2 conditions.

Next, $1\text{--}2.5 \times 10^8$ cells were harvested 1, 4, 12, 24, 36, 48 and 60 h after glucose addition as described earlier. Metabolites were extracted and measured by IC-MS as described earlier.

Data analysis was conducted with COMPOUND DISCOVERER (v.3.1, ThermoFisher Scientific) and the standard workflow for stable isotope labelling from COMPOUND DISCOVERER was chosen. The default settings, which are 5 ppm mass tolerance, 30% intensity tolerance and 0.1% intensity threshold for isotope pattern matching were used and the maximum exchange rate was set to 95%.

Results

Galdieria sulphuraria metabolizes several organic substrates

Previous work (Oesterhelt *et al.*, 2007) has suggested that *G. sulphuraria* is unable to grow mixotrophically in the presence of light plus organic carbon but rather alternates between heterotrophy (in the presence of an external source of organic carbon) and phototrophy (upon inorganic carbon consumption). This conclusion was based on experiments carried out at 25°C, i.e. a temperature that is far from the physiological optimum of this alga (above 40°C), and therefore decreases photosynthetic performances (Doemel & Brock, 1971; Ford, 1979; Rossoni & Weber, 2019; Rossoni *et al.*, 2019b). Thus, we decided to reinvestigate the possible occurrence of mixotrophy under conditions that resemble natural growth conditions (42°C, pH 2.0) in which *G. sulphuraria* displays maximum photosynthetic capacity.

First, we sought compounds that could improve algal growth in presence of light. We found that several hexoses, disaccharides and pentoses, but also some polyols and amino acids (L-alanine, L-glutamate) were able to boost *G. sulphuraria*'s growth when compared to strict photoautotrophic conditions (Fig. S1). Conversely, some organic acids (malic and citric acid) and amino acids (L-aspartate, L-leucine, L-valine, L-isoleucine, L-asparagine) had either no effect or led to a growth inhibition when compared to photoautotrophic conditions. Acetic acid was lethal to the cells. Compound concentrations were 25 mM, i.e. the same value employed in the study by Oesterhelt *et al.*, 2007. In the case of disaccharides, we reduced the concentration by a factor of two, to keep the overall carbon atoms concentration constant.

Based on these results, we focused on sorbitol, a compound that boosts growth in the dark without inducing a significant loss of photosynthetic pigments (Gross & Schnarrenberger, 1995). We confirmed that sorbitol was able to sustain cell division in the dark (Fig. 1), but its effect on growth was largely enhanced by a concomitant exposure to light. The final dry weight and number of cells collected at the end of the exponential phase in the light plus carbon condition (orange symbols, Fig. 1) exceeded the sum of cells obtained in the heterotrophic (black symbols, Fig. 1) plus the photoautotrophic (green symbols, Fig. 1) conditions. This finding indicates that *G. sulphuraria* is not only able to perform true mixotrophy under high temperature, dim light and presence of external organic carbon sources, but that this trophic mode is highly beneficial for its growth capacity. We obtained similar effects replacing sorbitol with a monosaccharide (glucose) and a disaccharide (saccharose) (Fig. S2).

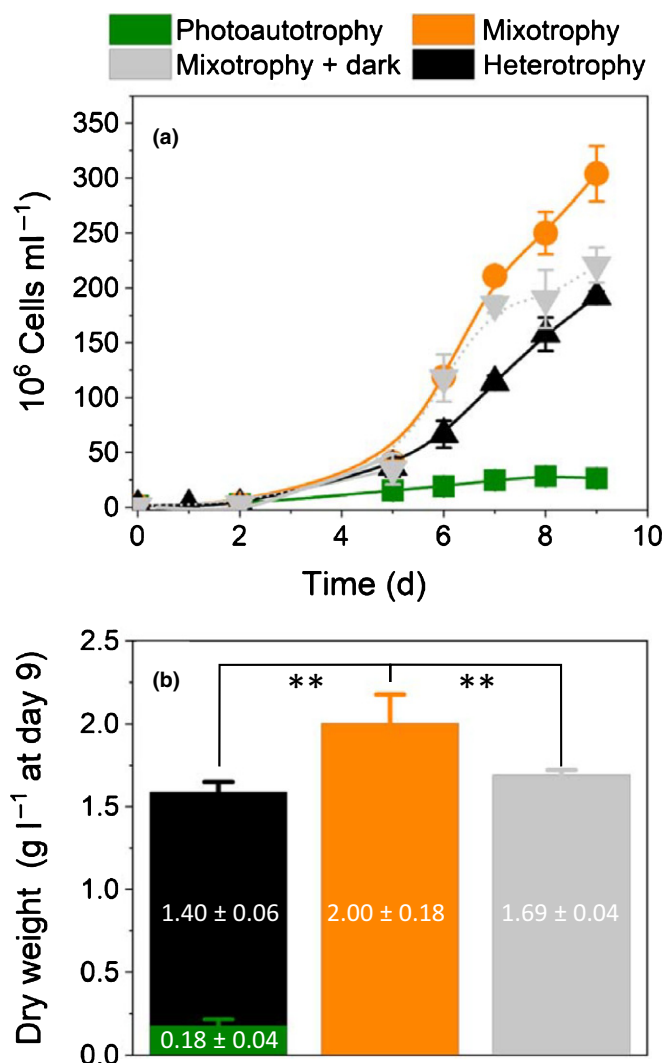


Fig. 1 Growth enhancement of *Galdieriasulphuraria* SAG21.92 by reduced carbon sources is light dependent. (a) Growth curves. Data from three biological replicates \pm SD. Error bars are shown when larger than the symbol size. *Galdieriasulphuraria* was grown in flasks at ambient CO₂ in photoautotrophic (light only, 30 μ mol photons m⁻² s⁻¹, green symbol), mixotrophic (30 μ mol photons m⁻² s⁻¹ plus D-sorbitol 25 mM, orange symbol) and heterotrophic (absence of light, presence of D-sorbitol 25 mM, black symbol). The initial cell concentration was 1.5×10^6 cells per milliliter. At day 5, the mixotrophic culture was split in two parts, and light was switched off in one culture (gray symbol). Growth was carried out at 42°C with shaking at 100 rpm, pH 2. (b) Dry weight estimated at day 9. Mixotrophic biomass (orange bar) exceeds the sum of photoautotrophic (green bar) and heterotrophic (black bar) biomass, highlighting the existence of a synergy under mixotrophic conditions. Data from three biological replicates \pm SD. **Indicates that at the 0.01 level the means of the two populations (mixotrophy on one side; heterotrophy + photoautotrophy on the other one) means are statistically different (ANOVA test). The concentration of inorganic nitrogen was 20 mM, while that of inorganic phosphate was 5 mM.

Respiration boosts photosynthesis in mixotrophic *Galdieria* cells

To further characterize the consequences of mixotrophy in *G. sulphuraria*, we transferred half of the cells grown in mixotrophy

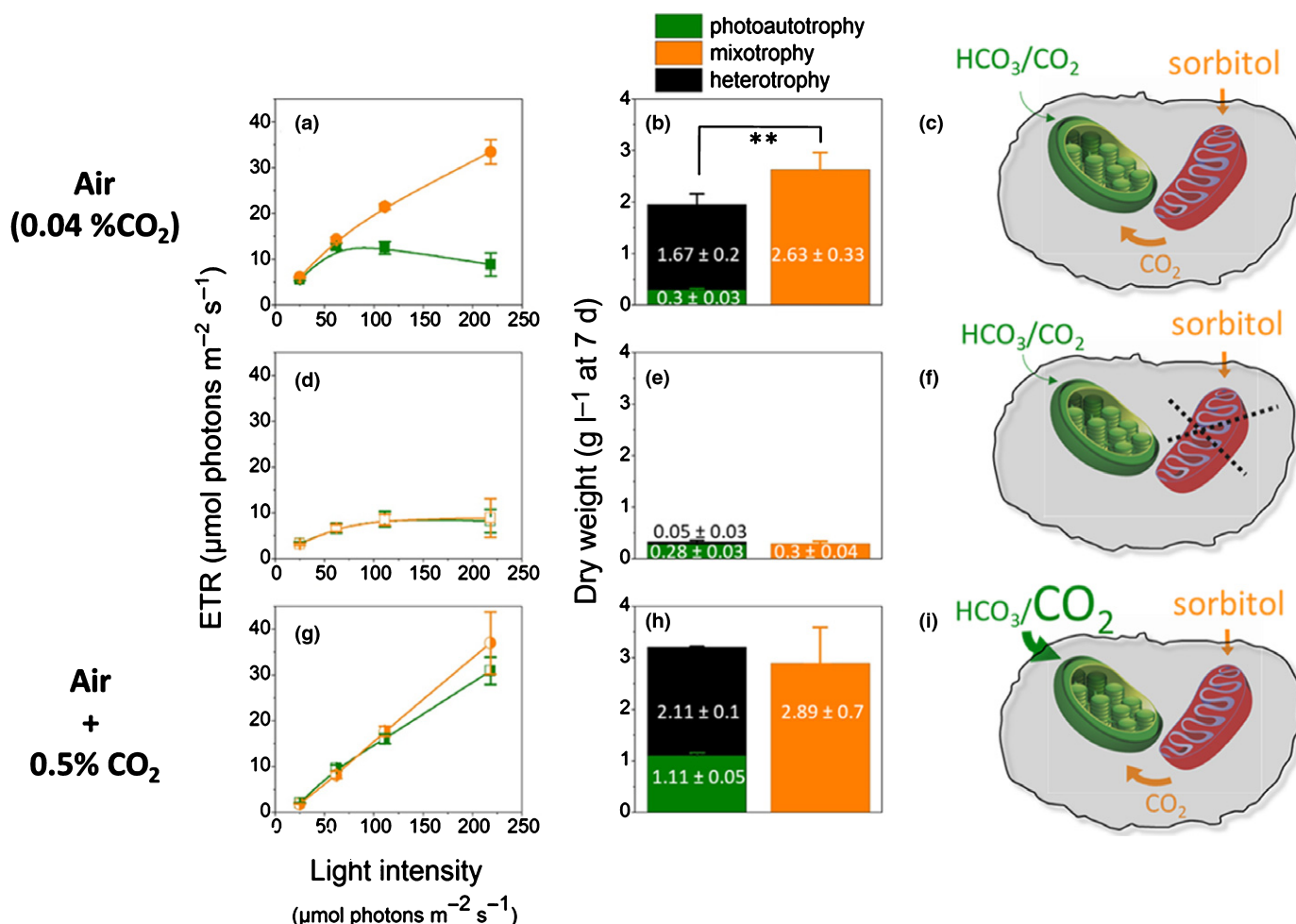
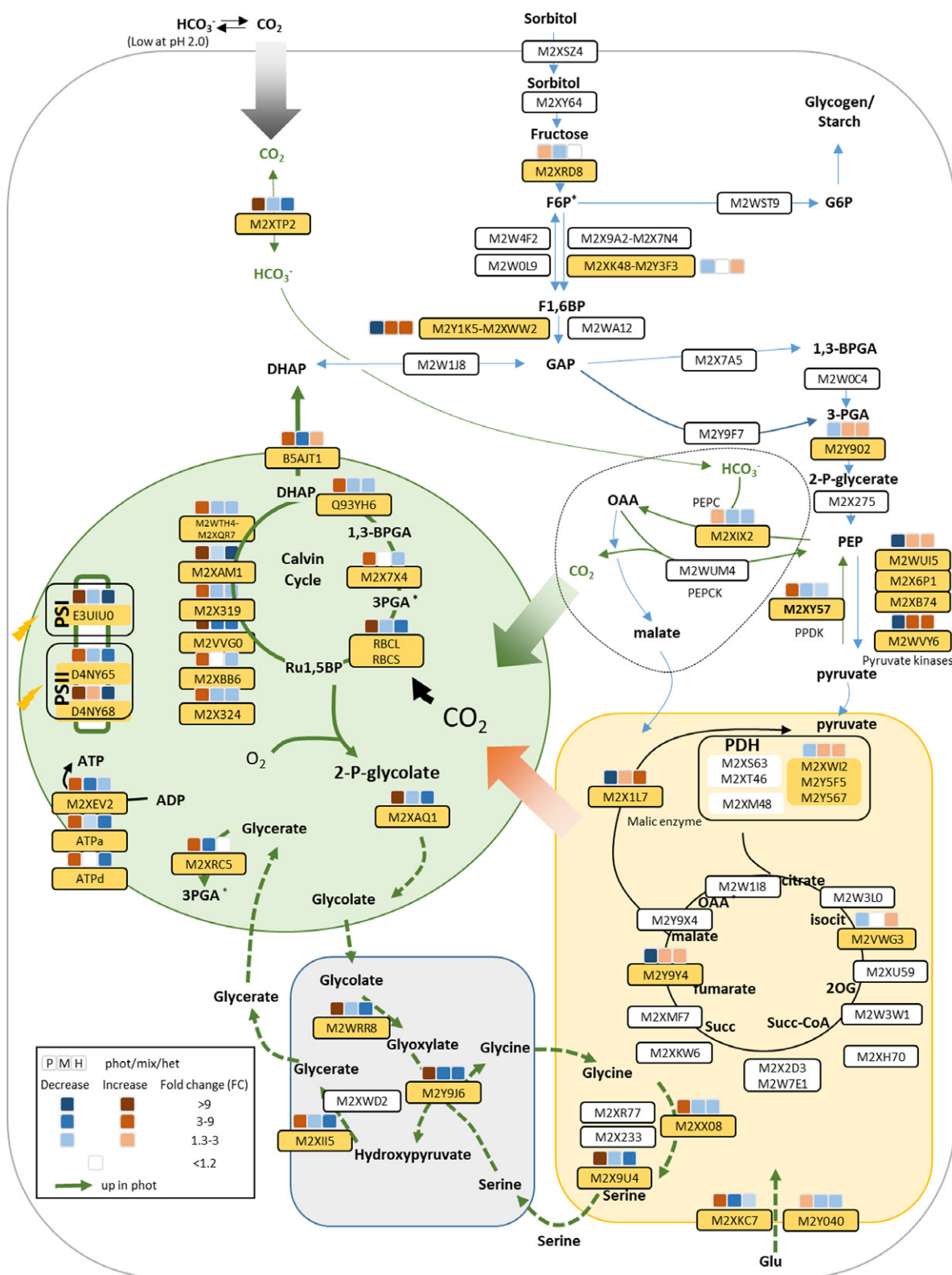


Fig. 2 *In situ* measurements of photosynthetic electron transfer rate (ETR) in photoautotrophic (light) and mixotrophic (light + 25 mM D-sorbitol) *Galdieriasulphuraria* SAG21.92 cells and biomass production. Cells were inoculated at 3.5×10^6 cell per milliliter and grown in a photobioreactor in the light (transmitted light $10 \mu\text{mol photons m}^{-2} \text{s}^{-1}$) and air before D-sorbitol was added in the absence (heterotrophy, black) and in the presence of light (mixotrophy, orange). Light was increased every day to keep the transmitted light to a constant value of $10 \mu\text{mol photons m}^{-2} \text{s}^{-1}$. Growth was followed at 42°C and pH 2. (a, d, g) After 5 d of growth (i.e. 2 d after the addition of D-sorbitol), ETR was measured directly on cultures within the photobioreactor, to avoid possible temperature stress. Measurements were done in air, in the absence (a, b) and presence (d, e) of respiratory inhibitors (SHAM (1 mM) and myxothiazol (10 μM), added 24 h before measurements), or in a CO_2 -enriched (0.5%) atmosphere (g, h). (a, d, g) Photosynthetic electron transfer: data from three biological replicates \pm SD. (b, e, h) Biomass production in photoautotrophic (green, data from 12 biological replicates \pm SD), heterotrophic (black, data from eight biological replicates \pm SD) and mixotrophic (orange, data from eight biological replicates \pm SD) conditions, respectively. Cells were collected after 7 d of growth (i.e. 4 d after addition of D-sorbitol). (c, f, i) Sketches representing possible CO_2 sources for photosynthesis in the three examined conditions. **Indicates that at the 0.01 level the means of the two populations (mixotrophy on one side; heterotrophy + photoautotrophy on the other one) means are statistically different (ANOVA test).

Fig. 3 Synthesis of proteomic changes between phototrophic, mixotrophic and heterotrophic growth conditions of *Galdieriasulphuraria* SAG21.92. Plastid is indicated in green, cytosol in white, mitochondrion in orange and peroxisome in gray. Proteins are identified by their SwissProt accessions; boxes on top of protein names represent fold-changes (protein average abundance in one condition was compared with the average abundance of the other two conditions – left photoautotrophy, middle mixotrophy, right heterotrophy). Proteins displaying statistically significant changes (see Methods section) are highlighted in yellow. They include proteins involved in CCM (pyruvate phosphate dikinase-M2XY57, carbonic anhydrase-M2XTP2, PEP carboxylase-M2XIX2), which are much more abundant in photoautotrophic conditions than in mixotrophic or heterotrophic conditions. Enzymes involved in photorespiration – dashed arrows – (phosphoglycolate phosphatase-M2XAQ1, glycolate oxidase-M2WRR8, serine-glyoxylate aminotransferase-M2Y9J6, glycine decarboxylase P proteins-M2X9U4, glycine/serine hydroxymethyltransferase-M2XX08, hydroxypyruvate reductase-M2XII5, glycerate kinase-M2XRC5) follow the same pattern as carbon concentrating mechanism (CCM) enzymes. Conversely, pyruvate kinases (especially M2WVY6) are strongly repressed under phototrophic condition, possibly to maintain a high PEP-oxaloacetate (OAA) pool for efficient fluxes in the carbon concentration cycle. Enzymes involved in photosynthesis are reduced under mixotrophic condition compared to photoautotrophic condition and strongly reduced under heterotrophic conditions. Mitochondrial respiratory proteins involved in the Krebs cycle or in ATP production are virtually not affected with the exception of fumarase and malic enzyme strongly reduced under phototrophic condition. Only representative proteins of the different complexes (e.g. photosynthesis, respiration) are represented. A more complete list of proteins can be found in Supporting Information Dataset S1. The complete set of proteomic data is available in Dataset S2.



for 5 d (Fig. 1) to heterotrophic condition and monitored growth of the four samples (photoautotrophic: green bar; heterotrophic: black bar; mixotrophic: orange bar; mixotrophic transferred to heterotrophy: gray bar) for another 5 d. While the mixotrophic

cells continued to display a higher growth capacity than the heterotrophic plus photoautotrophic ones, the mixotrophic cells transferred to the dark (gray symbols) slowly reached the same cell density (Fig. 1a) and dry weight (Fig. 1b) as the heterotrophic

culture, i.e. they lost the benefits provided by the simultaneous exposure to light and organic carbon within a few days. We conclude therefore that mixotrophy promotes a synergistic interaction between light and dark energy metabolisms, which slowly disappears when the light supply is halted.

In the experiments described earlier, photoautotrophic growth was most likely limited by the low light intensity ($30 \mu\text{mol photons m}^{-2} \text{s}^{-1}$), which was kept constant during growth, and therefore rapidly became limiting for photosynthesis when the cell concentration was increased in the flasks. Gas diffusion could also be limiting in flasks. Therefore, we repeated experiments in a photobioreactor (Fig. S3), where air bubbling ensured a more efficient gas delivery to the algae. Moreover, the intensity of the incident light was progressively increased in this setup to maintain a linear relationship between the cell number and the absorption. We reproduced the improvement of biomass productivity in mixotrophy with the photobioreactor (Fig. 2), where we could monitor biomass production and photosynthetic performances on actively growing cells using a custom-built fluorescence imaging setup to monitor photosynthesis via the ETR parameter (Maxwell & Johnson, 2000) (Fig. S3).

The ETR in the photoautotrophic cultures was lower than in mixotrophic ones (Fig. 2a). The difference was larger during the first days of culturing (Fig. S4, days 4 and 5, i.e. the first and second day after sorbitol addition), and then photosynthesis progressively diminished in the mixotrophic cells (Fig. S4, days 6 and 7, i.e. the third and fourth day of mixotrophy), where we also observed a large variability in the photosynthetic capacity (Fig. S4, day 7). We ascribe this variability to a differential consumption of sorbitol, and therefore of the mixotrophic synergistic effect, in the various samples. Consistent with this hypothesis, enhancement of photosynthesis was re-established in mixotrophic cultures, provided that sorbitol, nearly exhausted after 4 d (Fig. S5, day 7) was added again to the growth medium (Fig. S6).

To explain the synergistic effect of mixotrophy, we reasoned that photosynthesis could be limited by the availability of inorganic carbon in photoautotrophic cells. The latter is present only as CO_2 and at very low concentration ($10 \mu\text{M}$ (Gross *et al.*, 1998)) at ambient air in *G. sulphuraria*'s cultures, due to the acidic pH (pH 2). Mixotrophy could alleviate this limitation by providing extra CO_2 of mitochondrial origin via enhanced respiration (Figs 2c, S7). We tested this hypothesis by two approaches. First, we poisoned mixotrophic and photoautotrophic cultures with myxothiazol and SHAM, known inhibitors of the cyanide sensitive and insensitive respiratory pathways, respectively, and measured consequences on photosynthetic activity. Addition of these inhibitors completely abolished the enhancement of photosynthetic activity and of biomass productivity by mixotrophy (Fig. 2d–f). Next, we increased the CO_2 availability to the cells in mixotrophic cultures, to outcompete endogenous CO_2 of respiratory origin with an excess of exogenous inorganic carbon. As a prerequisite for this experiment, we calibrated the CO_2 requirement for optimum photosynthesis in our growth conditions (transmitted light of $10 \mu\text{mol photons m}^{-2} \text{s}^{-1}$). We found that photoautotrophic growth was increased by CO_2 up to a

concentration of 2% CO_2 (Fig. S8a), the apparent affinity for CO_2 being about 0.5%. Upon addition of external CO_2 , the photosynthetic capacity in photoautotrophic conditions increased and the biomass produced in heterotrophic plus photoautotrophic conditions became equal to that observed in mixotrophy (Fig. 2g–i). Overall, these data indicate that the synergy between respiration and photosynthesis is lost when the respiration is inhibited or when the photosynthesis becomes saturated with externally supplied CO_2 . Moreover, we hypothesize that photorespiration should be decreased to very low rates at saturating CO_2 , possibly contributing to the gain in biomass productivity at high CO_2 concentrations. In these experiments, we also observed that the amount of biomass produced by phototrophic cells supplemented with air was the same irrespective of the light intensity employed (Fig. S8b). Conversely, biomass production could be increased by increasing the light intensity in both phototrophic cells supplemented with 0.5% CO_2 (Fig. S8c) or in mixotrophic cells (Fig. S8d). These findings are fully consistent with the hypothesis that photosynthesis is CO_2 limited in air, and that this limitation can be alleviated by endogenous (mixotrophy) or exogenous CO_2 .

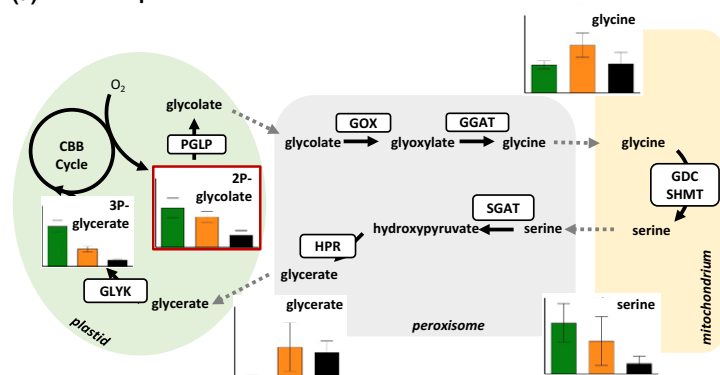
Metabolic acclimation to mixotrophy in *G. sulphuraria*

The observation that mixotrophy enhances photosynthesis to a similar level as upon addition of external CO_2 to *G. sulphuraria*, suggests that mixotrophy behaves as a strategy to traffic CO_2 from the mitochondria to the plastid, allowing this alga to successfully exploit all the energy resources available for growth and to minimize energy loss through photorespiration.

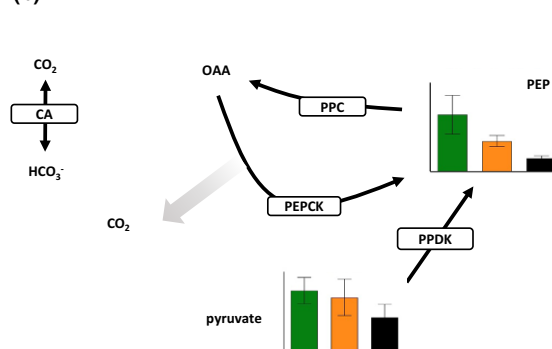
To substantiate this hypothesis, we performed a complete survey of the metabolic changes between the three trophic lifestyles, and relate these changes to modifications in the cell proteome. We found that photosynthetic proteins (complexes of the electron transfer chain, enzymes of the Calvin–Benson–Bassham cycle and transporters involved in triose phosphate export) were downregulated in mixotrophic conditions compared to photoautotrophic conditions (Fig. 3), in agreement with previous suggestions (Gross & Schnarrenberger, 1995; Oesterhelt *et al.*, 2007). Conversely, respiratory protein levels remained relatively constant in the three conditions. This observation (photosynthetic activity is enhanced in mixotrophy despite the downregulation of the photosynthetic machinery) fully supports the conclusion that intracellular increase in CO_2 due to enhanced respiratory activity more than compensates for the decrease in Rubisco (see also Fig. S9).

In line with the hypothesis that mixotrophy channels CO_2 from respiration to photosynthesis, proteomic analysis indicates that all the enzymes involved in photorespiration (phosphoglycolate phosphatase, glycolate oxidase, serine-glyoxylate aminotransferase, glycine decarboxylase, glycine/serine hydroxymethyltransferase, hydroxypyruvate reductase, glycerate kinase) were less abundant in mixotrophy. This is also true for Rubisco activase (Gasu_19410; Datasets S1, S2), an enzyme that was shown to be important under low CO_2 in *Chlamydomonas* (Pollock *et al.*, 2003). These findings are also

(a) Photorespiration



(b) C4-like CCM



(c) Upper glycolysis

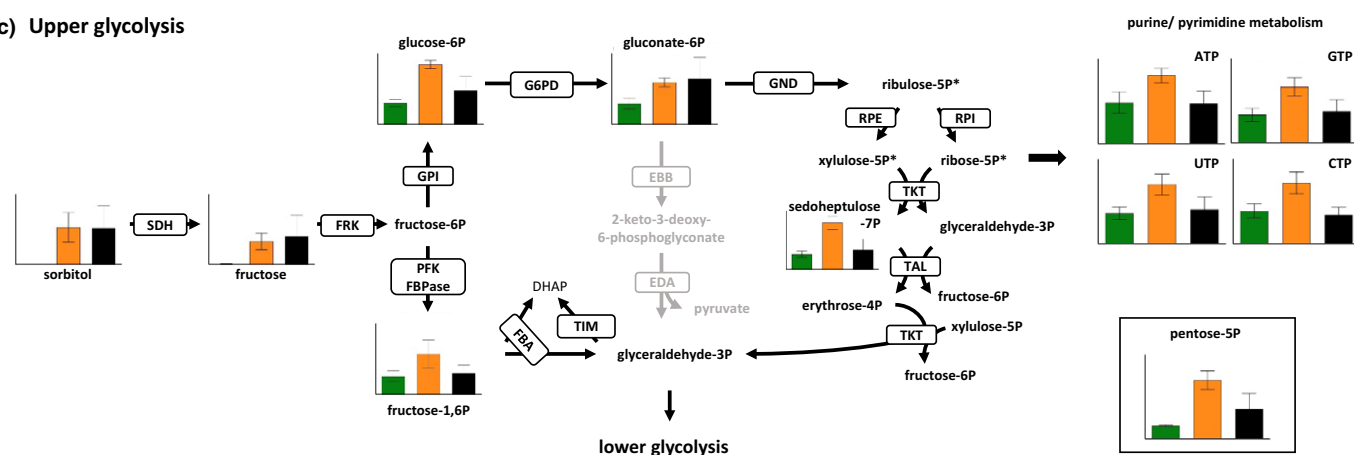


Fig. 4 Metabolic changes between phototrophic, mixotrophic and heterotrophic growth conditions of *Galdieriasulphuraria* SAG21.92. Non-phosphorylated metabolites were analyzed by gas chromatography-mass spectrometry (GC-MS), phosphorylated metabolites were analyzed using ion chromatography-mass spectrometry (IC-MS). Quantification of metabolites is provided in Supporting Information Dataset S3. Green bar: photoautotrophy; orange bar: mixotrophy; black bar: heterotrophy. (a) Changes of metabolites involved in photorespiration. 2P-glycolate as a photorespiration-specific metabolite is boxed in red. Glycolate, glycine, serine and glycerate are transported between cellular compartments as indicated by dashed arrows. PGLP: phosphoglycolate phosphatase; GOX: glycolate oxidase; GGAT: glutamate:glyoxylate aminotransferase; GDC: glycine decarboxylase complex; SHMT: serine hydroxymethyltransferase; SGAT: serine:glyoxylate aminotransferase; HPR: hydroxypyruvate reductase; GLYK: glycerate kinase. (b) Metabolites involved in a putative C4-type carbon concentrating mechanism (CCM). CA: carbonic anhydrase; PPC: phosphoenolpyruvate carboxylase; PEPCK: phosphoenolpyruvate carboxykinase; PDK: pyruvate phosphate dikinase; PEP: phosphoenolpyruvate. (c) Metabolic changes of intermediates of upper glycolytic pathways (EMP, ED, PPP) and purine/pyrimidine metabolism. The pentose-5P (ribulose-5P, xylulose-5P, ribose-5P, marked with an asterisk) could not be distinguished and are plotted in a single boxed graph. SDH: sorbitol dehydrogenase; FRK: fructokinase; GPI: glucose-6P isomerase; G6PD: glucose-6P dehydrogenase; GND: 6-phosphogluconate dehydrogenase; EBB: phosphogluconate dehydratase; EDA: KDPG aldolase; PFK: 6-phosphofructokinase; FBPase: fructose-1,6P biphosphatase; FBA: fructose biphosphatase aldolase; TIM: triosephosphate isomerase; RPE: ribulose-5P epimerase; RPI: ribulose-5P isomerase; TKT: transketolase; TAL: transaldolase. The full list of metabolite changes can be found in Dataset S3. The Y axes in the graphs correspond to normalized peak areas and error bars represent the standard deviation of biological quadruplicates.

corroborated by metabolite analysis (Fig. 4a). The amounts of the oxygenation product of Rubisco, 2-phosphoglycolate are highest under photoautotrophic conditions, lower in mixotrophic conditions, and very low in heterotrophic conditions. Glycine accumulates, likely due to a higher reduction potential inside the mitochondrial matrix under mixotrophic conditions, which will reduce the rate of oxidative decarboxylation of glycine by glycine decarboxylase. Consequently, the glycine to serine ratio was inverted compared to photoautotrophic conditions. The amounts of glycerate and 3-phosphoglycerate under mixotrophic conditions are mimicking those in heterotrophically grown cells (Fig. 4a).

Proteins involved in a putative C4-like carbon concentrating cycle (Rademacher *et al.*, 2017) (Figs 3, 4b) followed the same

pattern as the photorespiratory enzymes. Carbonic anhydrase and phosphoenolpyruvate carboxylase were more abundant under photoautotrophic conditions than under mixotrophic or heterotrophic conditions, and, in agreement with this finding, photoautotrophic cells also contained higher amounts of phosphoenolpyruvate (PEP) than mixotrophic or heterotrophic cells (Fig. 4b). The presence of this carbon concentrating cycle in photoautotrophic conditions could be supported by increased steady-state levels of phosphorylated C3 compounds, as suggested by the downregulation of pyruvate kinases in phototrophy (PEP consumption might be decreased) and strong induction of pyruvate ortho-phosphate dikinase (producing PEP). We assume that oxaloacetate (OAA) under photoautotrophic conditions is decarboxylated by PEP carboxykinase (PEPCK), and not after

reduction into malate by malate dehydrogenase and decarboxylation by mitochondrial malic enzyme. This hypothesis is supported by the finding that mitochondrial malic enzyme (ME) is strongly decreased in photoautotrophy (Fig. 3) and the malate pool size is smaller under this condition than in mixotrophy or heterotrophy. We note that decarboxylation by PEPCK (as compared to ME) is energy conserving and directly yields PEP for a new round of carboxylation by PEP carboxylase.

While part of the increase in biomass production in mixotrophic conditions can be attributed to the repression of photorespiration, other benefits of the mixotrophic lifestyle may come from more carbon units being shuttled into anabolic pathways. Indeed, we observed a general increase of metabolites of the oxidative pentose phosphate pathway (ribulose-5P, sedoheptulose-7P) and nucleoside triphosphates (adenosine triphosphate (ATP), guanosine triphosphate (GTP), uridine triphosphate (UTP), cytidine triphosphate (CTP)) as successor metabolites (Fig. 4c). The amounts do not differ between autotrophic and heterotrophic cultures but are clearly increased under mixotrophic conditions providing evidence for a higher flux of carbon at least into purine and pyrimidine synthesis.

Labeling experiments using carbon-13 (^{13}C)-labeled glucose, a sugar with similar effects on cell growth and biomass production as sorbitol (Fig. S2), further support this notion. We found a rapid incorporation of CO_2 from ^{13}C glucose into

photosynthetic metabolites, such as ribulose 1,5-bisphosphate (RuBP), sedoheptulose 1,7-bisphosphate (SBP), and 2-phosphoglycolate (2-PG) (Fig. 5). While RuBP also occurs in the oxidative pentose phosphate pathway, SBP and 2-PG are metabolites solely formed in the Calvin–Benson–Bassham cycle and can only carry a label when $^{13}\text{CO}_2$ released by respiration is fixed. Incorporation of the label by shuttling of carbon backbones from the cytosol into the chloroplast is unlikely since the solute transporters in the *G. sulphuraria*'s chloroplast envelope do not favor the import of glycolytic intermediates under photosynthetic conditions (Linka *et al.*, 2008). The rate of incorporation of ^{13}C is much reduced when external CO_2 levels are increased to 2%. Interestingly, the tricarboxylic acid cycle intermediate succinate exhibits a similar pattern of delayed labeling under high CO_2 conditions when compared to ambient air, indicating a slowed down glucose usage. Thus, the delay of label incorporation into the Calvin–Benson–Bassham cycle intermediates can be traced back to lower levels of labeled respiratory CO_2 under CO_2 saturated conditions.

Discussion

At variance with a previous report (Oesterheld *et al.*, 2007), *G. sulphuraria* cells are capable of a true mixotrophy, when transferred from strictly photoautotrophic conditions to a light and

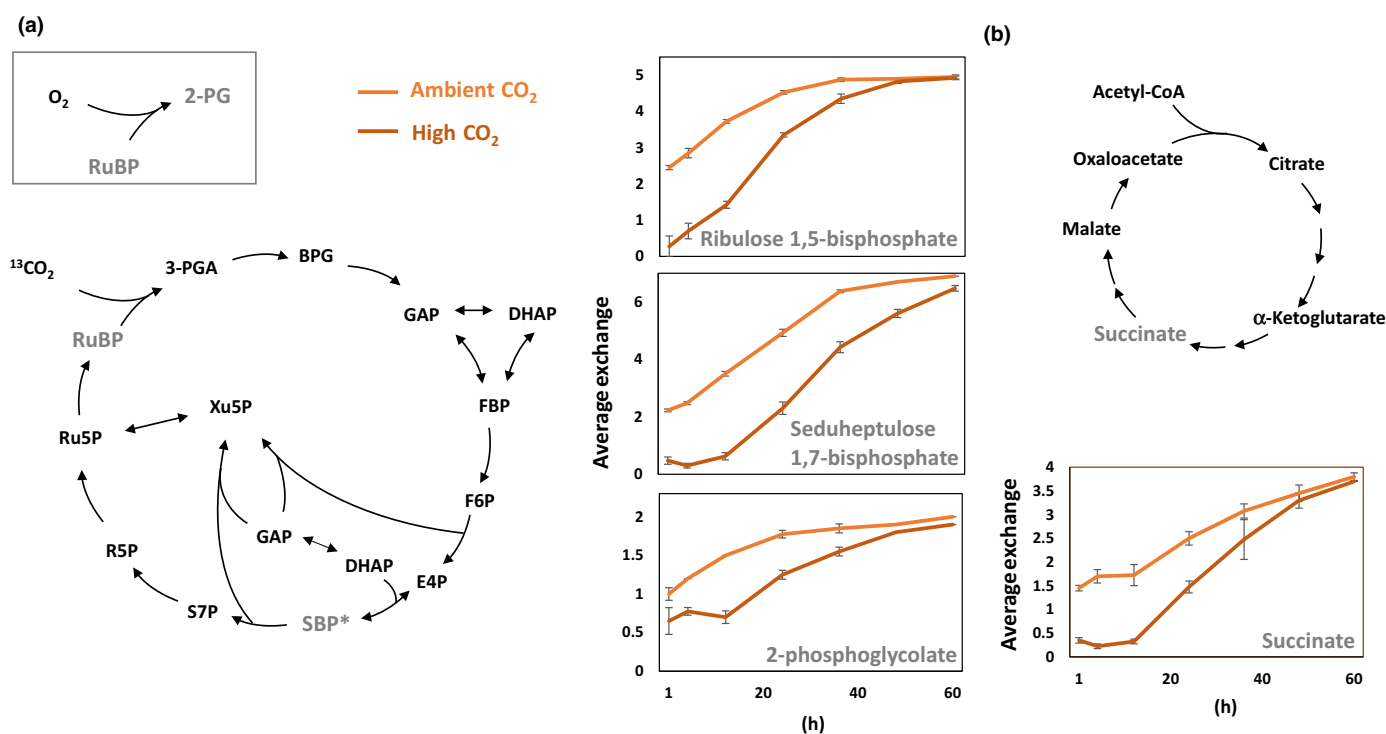


Fig. 5 Incorporation of carbon derived from carbon-13 (^{13}C)-labeled glucose into intermediates of the Calvin–Benson–Bassham (a) and tricarboxylic acid (b) cycles during mixotrophic cultivation of *Galdieriasulphuraria* SAG21.92 in two different CO_2 concentrations. Incorporation rates are displayed as average number of labeled carbon atoms in each molecule (average exchange). Error bars represent the standard deviation of biological quadruplicates. Light orange: cells grown in ambient air (0.02% CO_2). Dark orange cells grown in air supplied with 2% CO_2 . RuBP: ribulose 1,5-bisphosphate; 3-PGA: 3-phosphoglycerate; 2-PG: 2-phosphoglycolate; BPG: 1,3-bisphosphoglycerate; DHAP: dihydroxyacetone phosphate; GAP: glyceraldehyde 3-phosphate; FBP: fructose 1,6-bisphosphate; F6P: fructose 6-phosphate; E4P: erythrose 4-phosphate; Xu5P: xylulose 5-phosphate; SBP: sedoheptulose 1,7-bisphosphate; S7P: sedoheptulose 7-phosphate; R5P: ribose 5-phosphate; Ru5P: ribulose 5-phosphate.

organic carbon regime, provided that the temperature conditions are kept close to the ones experienced by this alga in its natural environment. This is not only true for the *G. sulphuraria* SAG21.92 strain used here, but also for *G. sulphuraria* 074G, i.e. the strain used in the previous study by Oesterhelt *et al.* (2007) when tested in the presence of the same external organic carbon sources employed here (see Fig. S10). Acclimation of the strictly photoautotrophic Cyanidiophyceae *Cyanidioschyzon merolae* to suboptimal growth temperatures of 25°C, led to massive rearrangements of the photosynthetic apparatus and a lower photon-to-oxygen conversion rate when compared to cells grown at 42°C (Nikolova *et al.*, 2017). Also, cultivation of *G. sulphuraria* at 25°C led to a downregulation of transcripts encoding components of the photosynthetic machinery (Rossoni *et al.*, 2019b). Therefore, cultivation at suboptimal temperatures may not be in favor of high photosynthetic rates and drive Cyanidiophyceae species capable of heterotrophic growth towards this trophic state.

Mixotrophy deeply alters the carbon metabolism of *G. sulphuraria* cells. Under photoautotrophic conditions, CO₂ is mainly concentrated by the PEPC/PEPCK driven CCM (Rademacher *et al.*, 2017). This process is repressed in mixotrophy. Moreover, enhanced respiration relieves the limitation of photosynthesis by inorganic carbon, which is at a low concentration (μmolar range) in the acid growth medium of this alga. We can quantify the extent of this process using the Clark electrode (as in Fig. S7) in a closed configuration, to avoid gas exchanges with the atmosphere (representative traces in Fig. S11a,c). In this case, the amount of O₂ produced by photosynthesis ($32.3 \pm 7.5 \mu\text{M}$ and $76.6 \pm 2 \mu\text{M}$ in photoautotrophy and mixotrophy, respectively) is commensurate with the amount of CO₂ available to Rubisco, i.e. the sum of respiratory CO₂ ($22 \pm 10.5 \mu\text{M}$ and $61 \pm 1.5 \mu\text{M}$ respectively, assuming a 1 : 1 stoichiometry with consumed O₂) plus the small CO₂ amount present in the medium (about 10 μM at pH 2) (Fig. S11c,d). These estimates clearly indicate that respiration in mixotrophy sets the rate of photosynthesis under limited CO₂ conditions. The proximity between mitochondria and chloroplasts (highlighted in red and green, respectively, in Fig. S12) may favor this process, facilitating intracellular gas exchange between the two cell organelles, as already shown in the case of other microalgae (Laverne, 1989).

At the same time, increased intracellular CO₂ concentration is expected to lower the rate of photorespiration in mixotrophy. Although the Rubisco enzymes from Cyanidiophyceae show some of the highest carboxylation specificities reported to date (Sugawara *et al.*, 1999), photorespiration is expected to proceed at high rates at the high temperatures and low CO₂ concentrations under which *Galdieria* grows. Indeed, knockout of peroxisomal glycolate oxidase in the transformable Cyanidiales alga *Cyanidioschyzon merolae* demonstrated that a functional photorespiratory pathway is essential for survival of these algae under ambient CO₂ concentrations (Rademacher *et al.*, 2016). The observed increase in the rate of photosynthesis and gain of biomass under high CO₂ and mixotrophic conditions ($25 \pm 6\%$, when combining data from Figs 1, 2) is consistent with

overcoming the expected loss of biomass gain due to photorespiration under photoautotrophic conditions.

In conclusion, by bypassing the possible metabolic antagonism between respiration and photosynthesis, *G. sulphuraria* can exploit the plethora of transporters encoded by its genome (Schonknecht *et al.*, 2013; Rossoni *et al.*, 2019a) and import organic carbon available in its environment and to boost CO₂ availability for photosynthesis. While this phenomenon certainly exists in other phototrophs (e.g. Rolland *et al.*, 1997), the capacity to enhance photosynthesis with respiratory CO₂ when the latter process is increased by exogenous carbon sources could be particularly relevant in *G. sulphuraria*. This alga thrives in an extreme environment, where growth is limited by low pH, high temperature and possibly light availability. Dissolved inorganic carbon is very low in this hot and acidic milieu (in fact its concentration inversely correlates with the pH of different collection sites in Yellowstone National Park) (Boyd *et al.*, 2012; Hamilton *et al.*, 2012) and its light-driven uptake is fairly low when compared to alkaline thermal habitats. Conversely, the concentration of dissolved organic carbon can be relatively high in the acidic hot springs (from 17 μM to 3 mM (Nye *et al.*, 2020)). Values could become much higher when this alga proliferates in mats (Gross *et al.*, 1998), where by-products of every group of microorganisms may serve as 'food' for other groups.

Based on these considerations, it is tempting to speculate that while photosynthesis should allow cells to colonize new environments devoid of any organic carbon source, the peculiar division mode of *G. sulphuraria* (formation of endospores associated with the release in the media of the mother cell wall remnants), may favor mixotrophy on a longer timescale. In the acidic conditions where *G. sulphuraria* lives, this material is probably rapidly hydrolyzed, providing an organic carbon source to the algae, along with other external sources for dissolved organic carbon, like e.g. high-temperature acid-digested wood (Nye *et al.*, 2020). Thanks to the abundance of transporters, this alga could outcompete other microorganisms such as fungi, which are also found in these extreme conditions, for growth. Thus, the coexistence of phototrophic, mixotrophic, and heterotrophic lifestyles thanks to the subtle compromise between the activity of the two energy-producing pathways (photosynthesis and respiration) would represent a key element for fitness and explain the success of *G. sulphuraria* to thrive in its extreme ecological niche. High fluctuations in the availability of dissolved organic and inorganic carbon, light, temperature, etc. in these environments possibly selected for the maintenance of a metabolic flexibility (Gross, 1999; Gross *et al.*, 2002; Ciniglia *et al.*, 2004; Cho *et al.*, 2020), which may have also allowed Cyanidiales to invade more moderate habitats (Yoon *et al.*, 2006; Azúa-Bustos *et al.*, 2009; Castenholz & McDermott, 2010) and to disperse over long distances to geographically isolated extreme habitats (Rossoni *et al.*, 2019a).

The same metabolic flexibility opens interesting perspectives to exploit this alga for biotechnology applications. *Galdieria sulphuraria* has already been employed in the fields of pigment/antioxidant production, bioremediation and bioenergy (Cizkova *et al.*, 2019) and the possibility to exploit its lifestyle flexibility

should be explored to cultivate this alga in organic matter-rich open ponds without contamination by other microorganisms.








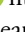





Acknowledgments

GC, DL, APMW, GF, MT, SB and MF acknowledge funds from the ANR (French Research Foundation) 'Momix' (Projet-ANR-17-CE05-0029). GC and GF also acknowledge support of the LabEX GRAL, ANR-10-LABX-49-01 financed within the University Grenoble Alpes graduate school (Ecoles Universitaires de Recherche) CBH-EUR-GS (ANR-17-EURE-0003). DDB acknowledged a PhD grant from CEA. JD was supported by the ATIP-Avenir program. CR and MC acknowledge the ARC grant (DARKMET proposal) for Concerted Research Actions (17/21-08), financed by the French Community of Belgium (Wallonia-Brussels Federation). This project received funding from the European Research Council: ERC Chloro-mito (grant no. 833184) to GC and GF. Metabolite analyses were supported by the CEPLAS Plant Metabolism and Metabolomics laboratory, which is funded by the Deutsche Forschungsgemeinschaft (DFG, German Research Foundation) under Germany's Excellence Strategy – EXC-2048/1 – project ID 390686111. MT, SB and MF acknowledge support from the ANR-funded French national infrastructure in biology and health ProFI (Proteomics French Infrastructure; ANR-10-INBS-08). The authors acknowledge the excellent technical assistance by E. Klemp, K. Weber and M. Graf for GC-MS and IC-MS measurements.

Author contributions

GC, DL, APMW and GF designed research; GC, DL, EG, PW, JJ, CH, SB, DDB, JD, BG, DF, MC and GF performed research; GC, DL, PW, MT, CR, MF, APMW and GF analyzed data; GC, DL, APMW and GF wrote the article.

ORCID

Sabine Brugière  <https://orcid.org/0000-0002-0757-0968>
 Michele Carone  <https://orcid.org/0000-0002-5561-0792>
 Gilles Curien  <https://orcid.org/0000-0002-5361-2399>
 Johan Decelle  <https://orcid.org/0000-0002-4343-8358>
 Denis Falconet  <https://orcid.org/0000-0001-8182-1182>
 Myriam Ferro  <https://orcid.org/0000-0002-4222-6847>
 Giovanni Finazzi  <https://orcid.org/0000-0003-0597-7075>
 Benoit Gallet  <https://orcid.org/0000-0001-8758-7681>
 Clément Hallopeau  <https://orcid.org/0000-0002-0692-2407>
 Dagmar Lyska  <https://orcid.org/0000-0002-9175-6334>
 Claire Remacle  <https://orcid.org/0000-0002-5016-9547>
 Marianne Tardif  <https://orcid.org/0000-0003-4438-8281>
 Andreas P.M. Weber  <https://orcid.org/0000-0003-0970-4672>

Data availability

The original contributions presented in the study are included in the article and in the Supporting Information and Supporting

Information datasets. Further inquiries can be directed to the corresponding author.

References

- Allen GJ. 1959. Studies with *Cyanidium caldarium*, an anomalously pigmented chlorophyte. *Archiv für Mikrobiologie* 32: 270–277.
- Avelange MH, Thiéry JM, Sarrey F, Gans P, Rébeillé F. 1988. Mass-spectrometric determination of O₂ and CO₂ gas exchange in illuminated higher-plant cells. *Planta* 183: 150–157.
- Azúa-Bustos A, González-Silva C, Mancilla RA, Salas L, Palma RE, Wynne JJ, McKay CP, Vicuña R. 2009. Ancient photosynthetic eukaryote biofilms in an Atacama Desert coastal cave. *Microbial Ecology* 58: 485–496.
- Barbier G, Oesterhelt C, Larson MD, Halgren RG, Wilkerson C, Garavito RM, Benning C, Weber APM. 2005. Comparative genomics of two closely related unicellular thermo-acidophilic red algae, *Galdieria sulphuraria* and *Cyanidioschyzon merolae*, reveals the molecular basis of the metabolic flexibility of *Galdieria sulphuraria* and significant differences in carbohydrate metabolism of both algae. *Plant Physiology* 137: 460–474.
- Barcyte D, Nedbalova L, Culka A, Kosek F, Jehlicka J. 2018. Burning coal spoil heaps as a new habitat for the extremophilic red alga *Galdieria sulphuraria*. *Fottea* 18: 19–29.
- Bhattacharya D, Yoon H, Hackett JD. 2003. Photosynthetic eukaryotes unite: endosymbiosis connects the dots. *BioEssays* 26: 50–60.
- Bogaert KA, Perez E, Rumin J, Giltay A, Carone M, Coosemans N, Radoux M, Eppe G, Levine RD, Remacle F *et al.* 2019. Metabolic, physiological, and transcriptomics analysis of batch cultures of the green microalga *Chlamydomonas* grown on different acetate concentrations. *Cells* 8: 1367.
- Bouchnak I, Brugiére S, Moyet L, Le Gall S, Salvi D, Kuntz M, Tardif M, Rolland N. 2019. Unraveling hidden components of the chloroplast envelope proteome: opportunities and limits of better MS sensitivity. *Molecular & Cellular Proteomics* 18: 1285–1306.
- Bouyssié D, Hesse A-M, Mouton-Barbosa E, Rompais M, Macron C, Carapito C, Gonzalez de Peredo A, Couté Y, Dupierri V, Burel A *et al.* 2020. Proline: an efficient and user-friendly software suite for large-scale proteomics. *Bioinformatics* 36: 3148–3155.
- Boyd ES, Fecteau KM, Havig JR, Shock EL, Peters JW. 2012. Modeling the habitat range of phototrophs in Yellowstone National Park: toward the development of a comprehensive fitness landscape. *Frontiers in Microbiology* 3: 221.
- Castenholz RW, McDermott TR. 2010. The cyanidiales: ecology, biodiversity, and biogeography. In: Seckbach J, Chapman DJ, eds. *Red algae in the genomic age*. Dordrecht, the Netherlands: Springer Netherlands, 357–371.
- Cecchin M, Benfatto S, Griggio F, Mori A, Cazzaniga S, Vitulo N, Delledonne M, Ballottari M. 2018. Molecular basis of autotrophic vs mixotrophic growth in *Chlorella sorokiniana*. *Scientific Reports* 8: 6465.
- Cho CH, Park SI, Ciniglia C, Yang EC, Graf L, Bhattacharya D, Yoon HS. 2020. Potential causes and consequences of rapid mitochondrial genome evolution in thermoacidophilic *Galdieria* (Rhodophyta) (vol 20, 112, 2020). *BMC Evolutionary Biology* 20: 112.
- Ciniglia C, Yoon HS, Pollio A, Pinto G, Bhattacharya D. 2004. Hidden biodiversity of the extremophilic Cyanidiales red algae. *Molecular Ecology* 13: 1827–1838.
- Cizkova M, Vitova M, Zachleder V. 2019. The red microalga *Galdieria* as a promising organism for applications in biotechnology. In: Vitová M ed. *Microalgae - From physiology to application*. London, UK: IntechOpen, 105–122.
- Combres C, Laliberté G, Reyssac JS, Delanoue J. 1994. Effect of acetate on growth and ammonium uptake in the microalga *Scenedesmus obliquus*. *Physiologia Plantarum* 91: 729–734.
- Cuaresma M, Janssen M, van den End EJ, Vilchez C, Wijffels RH. 2011. Luminostat operation: a tool to maximize microalgae photosynthetic efficiency in photobioreactors during the daily light cycle? *Bioresource Technology* 102: 7871–7878.
- Doemel WN, Brock TD. 1971. The physiological ecology of *Cyanidium caldarium*. *Journal of General Microbiology* 67: 17–32.

- Fang X, Wei C, Cai ZL, Fan O. 2004. Effects of organic carbon sources on cell growth and eicosapentaenoic acid content of *Nannochloropsis* sp. *Journal of Applied Phycology* 16: 499–503.
- Ferroni L, Giovanardi M, Poggioni M, Baldisserotto C, Pancaldi S. 2018. Enhanced photosynthetic linear electron flow in mixotrophic green microalga *Ettlia oleoabundans* UTEX 1185. *Plant Physiology and Biochemistry* 130: 215–223.
- Ford TW. 1979. Ribulose 1,5-bisphosphate carboxylase from the thermophilic, acidophilic alga, cyanidium-caldarium (geitler) – purification, characterization and thermostability of the enzyme. *Biochimica et Biophysica Acta (BBA) - Bioenergetics* 569: 239–248.
- Gemel J, Randall DD. 1992. Light regulation of leaf mitochondrial pyruvate-dehydrogenase complex – role of photorespiratory carbon metabolism. *Plant Physiology* 100: 908–914.
- Gross C. 1999. Revision of comparative traits for the acidophilic and thermophilic red algae Cyanidium and Galdieria. In: Seckbach J ed. *Enigmatic microorganisms and life in extreme environments*. Dordrecht, the Netherlands: Springer, 437–446.
- Gross W, Küver J, Tischendorf G, Bouchaala N, Büsch W. 1998. Cryptoendolithic growth of the red alga *Galdieria sulphuraria* in volcanic areas. *European Journal of Phycology* 33: 25–31.
- Gross W, Oesterhelt C. 1999. Ecophysiological studies on the red alga *Galdieria sulphuraria* isolated from southwest iceland. *Plant Biology* 1: 694–700.
- Gross W, Oesterhelt C, Tischendorf G, Lederer F. 2002. Characterization of a non-thermophilic strain of the red alga genus *Galdieria* isolated from Soos (Czech Republic). *European Journal of Phycology* 37: 477–483.
- Gross W, Schnarrenberger C. 1995. Heterotrophic growth of two strains of the acidophilic-thermophilic red alga *Galdieria sulphuraria*. *Plant & Cell Physiology* 36: 633–638.
- Gu J, Weber K, Klemp E, Winters G, Franssen SU, Wienpahl I, Huylmans A-K, Zecher K, Reusch TBH, Bornberg-Bauer E et al. 2012. Identifying core features of adaptive metabolic mechanisms for chronic heat stress attenuation contributing to systems robustness. *Integrative Biology* 4: 480–493.
- Hamilton TL, Vogl K, Bryant DA, Boyd ES, Peters JW. 2012. Environmental constraints defining the distribution, composition, and evolution of chlorophototrophs in thermal features of Yellowstone National Park. *Geobiology* 10: 236–249.
- Henkanatte-Gedera SM, Selvaratnam T, Karbakhsharavari M, Myint M, Nirmalakhandan N, Van Voorhies W, Lammers PJ. 2017. Removal of dissolved organic carbon and nutrients from urban wastewaters by *Galdieria sulphuraria*: laboratory to field scale demonstration. *Algal Research-Biomass Biofuels and Bioproducts* 24: 450–456.
- Hoefnagel MHN, Atkin OK, Wiskich JT. 1998. Interdependence between chloroplasts and mitochondria in the light and the dark. *Biochim Biophys Acta-Bioenergetics* 1366: 235–255.
- Iovinella M, Eren A, Pinto G, Pollio A, Davis SJ, Cennamo P, Ciniglia C. 2018. Cryptic dispersal of Cyanidiophytina (Rhodophyta) in non-acidic environments from Turkey. *Extremophiles* 22: 713–723.
- Johnson X, Alric J. 2012. Interaction between starch breakdown, acetate assimilation, and photosynthetic cyclic electron flow in *Chlamydomonas reinhardtii*. *Journal of Biological Chemistry* 287: 26445–26452.
- Johnson X, Vandystadt G, Bujaldon S, Wollman FA, Dubois R, Roussel P, Alric J, Beal D. 2009. A new setup for in vivo fluorescence imaging of photosynthetic activity. *Photosynthesis Research* 102: 85–93.
- Kromer S, Stitt M, Heldt HW. 1988. Mitochondrial oxidative phosphorylation participating in photosynthetic metabolism of a leaf cell. *FEBS Letters* 226: 352–356.
- Lavergne J. 1989. Mitochondrial responses to intracellular pulses of photosynthetic oxygen. *Proceedings of the National Academy of Sciences, USA* 86: 8768–8772.
- Linka M, Jamai A, Weber APM. 2008. Functional characterization of the plastidic phosphate translocator gene family from the thermo-acidophilic red alga *Galdieria sulphuraria* reveals specific adaptations of primary carbon partitioning in green plants and red algae. *Plant Physiology* 148: 1487–1496.
- Liu XJ, Duan SS, Li AF, Xu N, Cai ZP, Hu ZX. 2009. Effects of organic carbon sources on growth, photosynthesis, and respiration of *Phaeodactylum tricornutum*. *Journal of Applied Phycology* 21: 239–246.
- Martinez F, Orus MI. 1991. Interactions between glucose and inorganic carbon metabolism in *Chlorella vulgaris* strain UAM-101. *Plant Physiology* 95: 1150–1155.
- Maxwell K, Johnson GN. 2000. Chlorophyll fluorescence – a practical guide. *Journal of Experimental Botany* 51: 659–668.
- Merola A, Castaldo R, De Luca P, Gambardella R, Musachio A, Taddei R. 1981. Revision of *Cyanidium caldarium*. Three species of acidophilic algae. *Giornale botanico italiano* 115: 189–195.
- Moreira D, Lopezarchilla AI, Amils R, Marin I. 1994. Characterization of 2 new thermoacidophilic microalgae – genome organization and comparison with *Galdieria sulphuraria*. *FEMS Microbiology Letters* 122(1–2): 109–114.
- Nikolova D, Weber D, Scholz M, Bald T, Scharsack JP, Hippler M. 2017. Temperature-induced remodeling of the photosynthetic machinery tunes photosynthesis in the thermophilic alga *Cyanidioschyzon merolae*. *Plant Physiology* 174: 35–46.
- Nye JJ, Shock EL, Hartnett HE. 2020. A novel PARAFAC model for continental hot springs reveals unique dissolved organic carbon compositions. *Organic Geochemistry* 141: 103964.
- Oesterhelt C, Schmalzlin E, Schmitt JM, Lokstein H. 2007. Regulation of photosynthesis in the unicellular acidophilic red alga *Galdieria sulphuraria*. *The Plant Journal* 51: 500–511.
- Pärnik T, Keerberg O. 1995. Decarboxylation of primary and end products of photosynthesis at different oxygen concentrations. *Journal of Experimental Botany* 46: 1439–1477.
- Perrineau MM, Gross J, Zelzion E, Price DC, Levitan O, Boyd J, Bhattacharya D. 2014. Using natural selection to explore the adaptive potential of *Chlamydomonas reinhardtii*. *PLoS ONE* 9: e92533.
- Pollock SV, Colombo SL, Prout DL, Godfrey AC, Moroney JV. 2003. Rubisco activase is required for optimal photosynthesis in the green alga *Chlamydomonas reinhardtii* in a low-CO₂ atmosphere. *Plant Physiology* 133: 1854–1861.
- Rademacher N, Kern R, Fujiwara T, Mettler-Altmann T, Miyagishima SY, Hagemann M, Eisenhut M, Weber APM. 2016. Photorespiratory glycolate oxidase is essential for the survival of the red alga *Cyanidioschyzon merolae* under ambient CO₂ conditions. *Journal of Experimental Botany* 67: 3165–3175.
- Rademacher N, Wrobel TJ, Rossoni AW, Kurz S, Brautigam A, Weber APM, Eisenhut M. 2017. Transcriptional response of the extremophile red alga *Cyanidioschyzon merolae* to changes in CO₂ concentrations. *Journal of Plant Physiology* 217: 49–56.
- Reeb V, Bhattacharya D. 2010. The thermo-acidophilic Cyanidiophyceae (Cyanidiales). In: Seckbach J, Chapman D, eds. *Red algae in the genomic age. Cellular origin, life in extreme habitats and astrobiology, vol. 13*. Dordrecht, the Netherlands: Springer, 409–426.
- Rolland N, Dorne AJ, Amoroso G, Sultemeyer DF, Joyard J, Rochaix JD. 1997. Disruption of the plastid ycf10 open reading frame affects uptake of inorganic carbon in the chloroplast of *Chlamydomonas*. *EMBO Journal* 16: 6713–6726.
- Rossoni AW, Price DC, Seger M, Lyska D, Lammers P, Bhattacharya D, Weber APM. 2019a. The genomes of polyextremophilic cyanidiales contain 1% horizontally transferred genes with diverse adaptive functions. *Elife* 8: e45017.
- Rossoni AW, Schonknecht G, Lee HJ, Rupp RL, Flachbart S, Mettler-Altmann T, Weber APM, Eisenhut M. 2019b. Cold Acclimation of the thermoacidophilic red alga *Galdieria sulphuraria*: Changes in gene expression and involvement of horizontally acquired genes. *Plant & Cell Physiology* 60: 702–712.
- Rossoni AW, Weber APM. 2019. Systems biology of cold adaptation in the polyextremophilic red alga *Galdieria sulphuraria*. *Frontiers in Microbiology* 10: 927.
- Schmidt RA, Wiebe MG, Eriksen NT. 2005. Heterotrophic high cell-density fed-batch cultures of the phycocyanin-producing red alga *Galdieria sulphuraria*. *Biotechnology and Bioengineering* 90: 77–84.
- Schonknecht G, Chen W-h, Ternes C, Barbier Gg, Shrestha Rp, Stanke M, Brautigam A, Baker Bj, Banfield Jf, Garavito Rm et al. 2013. Gene transfer from bacteria and archaea facilitated evolution of an extremophilic eukaryote. *Science* 339: 1207–1210.
- Schwaiger M, Rampler E, Hermann G, Miklos W, Berger W, Koellensperger G. 2017. Anion-exchange chromatography coupled to high-resolution Mass

- Spectrometry: a powerful tool for merging targeted and non targeted metabolomics. *Analytical Chemistry* 89: 7667–7674.
- Shim SH, Lee SK, Lee DW, Brilhaus D, Wu G, Ko S, Lee CH, Weber APM, Jeon JS. 2020. Loss of function of rice plastidic glycolate/glycerate translocator 1 impairs photorespiration and plant growth. *Frontiers in Plant Science* 10: 1726.
- Sugawara H, Yamamoto H, Shihata N, Inoue T, Okada S, Miyake C, Yokota A, Kai Y. 1999. Crystal structure of carboxylase reaction-oriented ribulose 1,5-bisphosphate carboxylase oxygenase from a thermophilic red alga, *Galdieria partita*. *Journal of Biological Chemistry* 274: 15655–15661.
- Tcherkez G, Bligny R, Gout E, Mahe A, Hodges M, Cornic G. 2008. Respiratory metabolism of illuminated leaves depends on CO₂ and O₂ conditions. *Proceedings of the National Academy of Sciences, USA* 105: 797–802.
- Villanova V, Fortunato AE, Singh D, Dal Bo D, Conte M, Obata T, Jouhet J, Fernie AR, Marechal E, Falcione A *et al.* 2017. Investigating mixotrophic metabolism in the model diatom *Phaeodactylum tricornutum*. *Philosophical Transactions of the Royal Society of London. Series B: Biological Sciences* 372: 20160404.
- Wan MX, Liu P, Xia JL, Rosenberg JN, Oyler GA, Betenbaugh MJ, Nie ZY, Qiu GZ. 2011. The effect of mixotrophy on microalgal growth, lipid content, and expression levels of three pathway genes in *Chlorella sorokiniana*. *Applied Microbiology and Biotechnology* 91: 835–844.
- Wieczorek S, Combes F, Lazar C, Gianetto QG, Gatto L, Dorffer A, Hesse AM, Coute Y, Ferro M, Bruley C *et al.* 2017. DAPAR & ProStaR: software to perform statistical analyses in quantitative discovery proteomics. *Bioinformatics* 33: 135–136.
- Wieczorek S, Combes F, Borges H, Burger T. 2019. Protein-level statistical analysis of quantitative label-free proteomics data with ProStaR. *Methods in Molecular Biology* 1959: 225–246.
- Xu F, Hu HH, Cong W, Cai ZL, Ouyang F. 2004. Growth characteristics and eicosapentaenoic acid production by *Nannochloropsis* sp. in mixotrophic conditions. *Biotechnology Letters* 26: 51–53.
- Yoon HS, Ciniglia C, Wu M, Cameron JM, Pinto G, Pollio A, Bhattacharya D. 2006. Establishment of endolithic populations of extremophilic Cyanidiales (Rhodophyta). *BMC Evolutionary Biology* 6: 78.
- Yoon H, Hackett JD, Pinto G, Bhattacharya D. 2002. The single, ancient origin of chromist plastids. *Proceedings of the National Academy of Sciences, USA* 99: 15507–15512.
- Yoon H, Hackett JD, Ciniglia C, Pinto G, Bhattacharya D. 2004. A molecular timeline for the origin of photosynthetic eukaryotes. *Molecular Biology and Evolution* 21: 809–818.

Supporting Information

Additional Supporting Information may be found online in the Supporting Information section at the end of the article.

Dataset S1 Proteins involved in photosynthesis, central metabolism and respiration were selected from the complete proteomic dataset (see Dataset S2) and used to build Fig. 3.

Dataset S2 Compared proteomic analysis between photoautotrophic, mixotrophic and heterotrophic growth conditions.

Dataset S3 Compared metabolomic analysis between photoautotrophic, mixotrophic and heterotrophic growth conditions.

Fig. S1 Consequences of different substrates on *Galdieria sulphuraria* growth in the light.

Fig. S2 *Galdieria sulphuraria* growth in photoautotrophic, mixotrophic and heterotrophic conditions driven by a polyol, an hexose and a disaccharide.

Fig. S3 Experimental setup to expose cells to a constant photons/cell ratio.

Fig. S4 *In situ* measurements of photosynthetic electron transfer rate (ETR) in photoautotrophic (light) and mixotrophic (light + 25 mM D-sorbitol) cells.

Fig. S5 Enhancement of cell growth by mixotrophy and sorbitol consumption in *Galdieria sulphuraria*.

Fig. S6 Mixotrophy is restored in *Galdieria sulphuraria* upon addition of a carbon source.

Fig. S7 Respiration and net photosynthesis were measured every day in the three different growth conditions (photoautotrophy, mixotrophy and heterotrophy).

Fig. S8 Biomass production as a function of transmitted light intensity and CO₂ concentration.

Fig. S9 Immunodetection of Rubisco in phototrophic and mixotrophic cultures under ambient and enhanced CO₂ atmosphere.

Fig. S10 Comparative analysis of phototrophic, mixotrophic and heterotrophic performances in *Galdieria sulphuraria* 074G and SAG21.92 species with D-sorbitol and D-glucose.

Fig. S11 Respiration fuels photosynthesis in photoautotrophic and mixotrophic *Galdieria sulphuraria* cultures.

Fig. S12 Transmission electron microscopy of *Galdieria sulphuraria* SAG21.92 grown 5 d under photoautotrophic, mixotrophic and heterotrophic conditions.

Methods S1 Microalgae and media composition, growth, cell fresh weight and dry weight estimates, Clark electrode oxygen and photophysiology measurements, mass spectrometry-based proteomic analyses, metabolic analyses by IC-MS, electron microscopy sample preparation and observation.

Please note: Wiley Blackwell are not responsible for the content or functionality of any Supporting Information supplied by the authors. Any queries (other than missing material) should be directed to the *New Phytologist* Central Office.